Regenerative Therapy 27 (2024) 354–364

Contents lists available at ScienceDirect

Regenerative Therapy

journal homepage: http://www.elsevier.com/locate/reth

Original Article

Mesenchymal stem cell-derived extracellular vesicles relieve endothelial cell senescence via recovering CTRP9 upon repressing miR-674-5p in atherosclerosis

Min Zeng [a, *, 1], Yangli He [a, 1], Yali Yang [b], Mengdi Wang [b], Yue Chen [b], Xin Wei [c, **]

[a] Medical Center, Hainan Affiliated Hospital of Hainan Medical University (Hainan General Hospital), Haikou 570311, Hainan Province, PR China
[b] Hainan Medical University, Haikou 570311, Hainan Province, PR China
[c] Department of Otolaryngology Head and Neck Surgery, Hainan Affiliated Hospital of Hainan Medical University (Hainan General Hospital), Haikou 570311, Hainan Province, PR China

ARTICLE INFO

Article history:
Received 17 November 2023
Received in revised form
14 March 2024
Accepted 24 March 2024

Keywords:
Atherosclerosis
ADSC-EVs
miR-674-5p
CTRP9
Endothelial cell senescence

ABSTRACT

Background: The senescence of endothelial cells is of great importance involving in atherosclerosis (AS) development. Recent studies have proved the protective role of mesenchymal stem cell-derived extracellular vesicles in AS, herein, we further desired to unvei their potential regulatory mechanisms in endothelial cell senescence.

Methods: Senescence induced by H_2O_2 in primary mouse aortic endothelial cells (MAECs) was evaluated by SA-β-gal staining. Targeted molecule expression was detected by qRT-PCR and Western blotting. The biological functions of MAECs were determined by CCK-8, flow cytometry, transwell, and tube formation assays. Oxidative injury was assessed by LDH, total and lipid ROS, LPO and MDA levels. The proliferation of adipose-derived mesenchymal stem cell (ADSCs) was analyzed by EdU assay. Effect of ADSCs-derived extracellular vesicles (ADSC-EVs) on AS was investigated in HFD-fed *ApoE*$^{-/-}$ mice.

Results: miR-674-5p was up-regulated, while C1q/TNF-related protein 9 (CTRP9) was down-regulated in H_2O_2-induced senescent MAECs. CTRP9 was demonstrated as a target gene of miR-674-5p. miR-674-5p inhibition restrained senescence, oxidative stress, promoted proliferation, migration, and angiogenesis of H_2O_2-stimulated MAECs via enhancing CTRP9 expression. Moreover, treatment with ADSC-EVs inhibited H_2O_2-induced senescence and dysfunction of MAECs through regulating miR-674-5p/CTRP9 axis. In the *in vivo* AS mouse model, ADSC-EVs combination with miR-674-5p silencing slowed down AS progression via up-regulation of CTRP9.

Conclusion: ADSC-EVs repressed endothelial cell senescence and improved dysfunction via promotion of CTRP9 expression upon miR-674-5p deficiency during AS progression, which might provide vital evidence for ADSC-EVs as a promising therapy for AS.

Abbreviations: AS, atherosclerosis; MAECs, mouse aortic endothelial cells; ADSCs, adipose-derived mesenchymal stem cells; ADSC-EVs, ADSCs-derived extracellular vesicles; CTRP9, C1q/TNF-related protein 9; MSCs, mesenchymal stem cells; miRNAs, microRNAs; SA-β-gal, senescence-asociated-β-glactosidase; qRT-PCR, quantitative real-time polymerase chain reaction; WT, wild type; MUT, mutant; TEM, transmission electron microscope; sh-CTRP9, shRNA targeting CTRP9; CCK-8, cell counting kit-8; EdU, 5-Ethynyl-2′-deoxyuridine; LDH, lactate dehydrogenase; LPO, lipid peroxide; MDA, malondialdehyde; ROS, reactive oxygen species; HFD, high-fat diet; TG, triglycerides; TC, total cholesterol; LDL-C, low-density lipoprotein; HE, hematoxylin-eosin; SD, standard deviation; 3′UTR, 3′untranslated regions.

* Corresponding author. Medical Center, Hainan Affiliated Hospital of Hainan Medical University (Hainan General Hospital), No. 19, Xiuhua Road, Xiuying District, Haikou 570311, Hainan Province, PR China.

** Corresponding author. Department of Otolaryngology Head and Neck Surgery, Hainan Affiliated Hospital of Hainan Medical University (Hainan General Hospital), No. 19, Xiuhua Road, Xiuying District, Haikou 570311, Hainan Province, PR China.

E-mail addresses: hndzm6@126.com (M. Zeng), hnweking@sina.com (X. Wei).

Peer review under responsibility of the Japanese Society for Regenerative Medicine.

[1] Min Zeng and Yangli He are co-first authors.

https://doi.org/10.1016/j.reth.2024.03.027

1. Introduction

Atherosclerosis (AS) is an aging-associated inflammatory disorder of the vascular system featured by atheroma formation in the arteries, which remains the primary cause of cardiovascular and cerebrovascular diseases and has high morbidity and mortality worldwide [1]. Depending on disease severity, therapeutic strategies for AS include acute, common, drug-based therapies, and surgery [2–4]. Although the therapeutic methods for AS are continuously improving, there is still a high mortality for AS patients at high risk [5]. Thus, identification of novel therapies for AS is still highly required.

As key components of the vascular inner layer, vascular endothelial cells are responsible for maintaining vascular homeostasis [6]. However, during aging-induced vascular dysfunctions, senescent endothelial cells may lose vascular repair ability, thus decreasing endothelial-dependent vasomotor function [7]. Endothelial cell senescence has been recognized as a crucial mediator for vascular aging-associated disease, including AS [8]. It has been reported that endothelial cell senescence leads to endothelial barrier dysfunction as a result of endothelial erosion during AS progression [9]. Therefore, inhibition of endothelial senescence represents a therapeutic strategy for preventing atherosclerotic lesion. So far, the effective interventions for preventing endothelial cell senescence during AS development are limited.

C1q/TNF-related protein 9 (CTRP9) is a novel identified adiponectin, possessing anti-inflammatory capacities [10]. Growing evidence has proved that CTRP9 exerts protection against obesity, and diabetes that are risk factors for AS [11,12]. Recent studies indicated that CTRP9 could attenuate AS via repressing inflammation, lipogenesis, and endothelial dysfunction, suggesting CTRP9 as a potential treatment target for AS [13–15]. Although the therapeutic action of CTRP9 on AS has been documented, the exact mechanisms underlying CTRP9 regulation still need to be clarified.

Mesenchymal stem cells (MSCs) have been considered as beneficial cells as a regenerative treatment choice for AS [16]. MSCs can be isolated from multiple sources, including adipose tissue. It has recognized that the biological functions of MSCs are associated with their paracrine activity through extracellular vehicles (EVs) release [17]. EVs can carry various functional constituents, including proteins and microRNAs (miRNAs), which elicit powerful biological effects. MSCs-derived EVs have been reported to exhibit anti-atherosclerotic roles, which were similar to their parent cells [18]. Notably, CTRP9 is a secretory protein that mainly produced by adipose tissue [19]. Thus, we speculated that EVs from adipose-derived MSCs (ADSC-EVs) might mitigate AS progression via delivering CTRP9 protein.

This study explored whether ADSC-EVs suppressed endothelial cell senescence via releasing CTRP9 protein and its up-stream modulatory mechanisms in AS model. We found that CTRP9 was targeted by miR-674-5p. miR-674-5p inhibition promoted CTRP9 expression, thereby suppressing endothelial cell senescence. Moreover, ADSC-EVs restrained senescence and restored biological functions of endothelial cells by enhancing CTRP9 expression. ADSC-EVs combined with miR-674-5p inhibition effectively ameliorated AS development via CTRP9 up-regulation. In summary, our current findings suggest that miR-674-5p inhibition in combination with ADSC-EVs might be an effective therapy for AS.

2. Methods

2.1. Ethic statement

The animal procedures were conducted in compliance with the Directive 2010/63/EU of the European Parliament on animal protection and approved by the Ethic Committee of Hainan Affiliated Hospital of Hainan Medical University (Hainan General Hospital).

2.2. Isolation of mouse aortic endothelial cells (MAECs) and treatment

Primary MAECs were isolated from C57BL/6J mice (Slac Jingda Laboratory Animal Co., Ltd, Hunan, China) as previously described [20]. In brief, the mice were anesthetized to obtain the abdominal aorta, followed by cutting into 1 mm pieces. The aortic segments were maintained on matrix for 3 d. Then, the MAECs were passaged and cultured with endothelial cell growth medium at 37 °C with 5% CO_2. MAECs at 2–3 passages were adopted in this study.

The primary MAECs were stimulated with various concentrations of H_2O_2 (0, 25, 50, and 100 μM) for 24 h for the evaluation of senescence.

2.3. Immunofluorescence staining

For characterization of MAECs, cells were fixed with 10% formalin for 30 min. After treatment with 0.4% Triton X-100 and 3% BSA for 30 min, MAECs were probed with anti-CD31 antibody (1:50, A0378, ABcolnal, Wuhan, China) at 4 °C overnight. The cells were incubated with Cy3 Goat Anti-Rabbit IgG (1:100, AS007, ABcolnal) for 1 h. Finally, the MAECs were stained DAPI and examined using a fluorescence microscope (Olympus, Japan).

2.4. Senescence-asociated-β-glactosidase (SA-β-gal) staining

To evaluate MAEC senescence, the treated cells were fixed with fixative solution for 15 min, and stained using the Senescence β-Galactosidase Staining Kit (Beyotime, Haimen, China) at 37 °C overnight in the absence of CO_2. The stained MAECs were observed under a light microscope.

2.5. Quantitative real-time polymerase chain reaction (qRT-PCR)

Total RNA was isolated from MAECs or aortas using the miRNeasy Kit (Qiagen, Germany) and reverse-transcribed into cDNA using the PrimeScript RT Reagent Kit (Takara, Japan). The PCR amplification was conducted using the quantitative SYBR Green RT-PCR kit (Qiagen). Relative expression of genes normalized to U6 or GAPDH was calculated by the $2^{-\Delta\Delta Ct}$ method. The primers used in this study were listed in Table 1.

2.6. Western blotting

Total proteins were extracted using the RIPA buffer (Beyotime) and the protein concentration was detected using the BCA assay kit (Thermo Fisher, USA). Protein samples (30 μg) were subjected to SDS-PAGE, and blotted onto polyvinylidene fluoride membranes. After blocking in 5% non-fat milk, the membranes were incubated primary antibodies against CTRP9 (1:500, NBP2-46834, Novus

Table 1
Primer sequences for RT-qPCR.

Gene	Forward (5′-3′)	Reverse (5′-3′)
miR-674-5p	GCGGCGGGCACTGAGATGGGAG	ATCCAGTGCAGGGTCCGAGG
P16	CGAACTCGAGGAGAGCCATC	TACGTGAACGTTGCCCATCA
P21	TAAGGACGTCCCACTTTGCC	AAAGTTCCACCGTTCTCGGG
P53	AAACGCTTCGAGATGTTCCG	CAAGGCTTGGAAGGCTCTAGG
LMNB1	GAGGAGGAGGAGGAG	CAAGTTCACATAATGCCACAG
U6	TCGCTTCGGCAGCACATA	GGGCCATGCTAAATCTTCTC
GAPDH	GGTGAAGGTCGGTGTGAACG	CTCGCTCCTGGAAGATGGTG

Biologicals, USA), TSG101 (1:500, A1692, ABcolnal), CD63 (1:100, A5271, ABcolnal), Calnexin (ab22595, 1:1000, Abcam, UK), GAPDH (1:10,000, A19056, ABcolnal) at 4 °C overnight, followed by incubation with HRP Goat Anti-Rabbit IgG (H + L) (1:2000, AS014, ABcolnal) for 1 h. The protein bands were visualized with the ECL luminescence reagent (Sangon, Shanghai, China).

2.7. Dual luciferase reporter assay

The wild type (WT) sequences of the CTRP9 3′-UTR containing the putative miR-674-5p binding sites or mutant (MUT) sequences were inserted into the psiCHECK-2 vector (Promega, USA). The constructed vectors together with miR-674-5p mimic or mimic NC (GenePharma, Shanghai, China) were transfected into HEK-293T cells. The Dual-Lucy Assay Kit (Solarbio, Beijing, China) was used to determine the relative luciferase activity.

2.8. Extraction, culture, and characterization of ADSCs

Primary ADSCs were extracted from the adipose tissues in the inguinal region of C57BL/6 mice according to a previous study [21]. Briefly, the adipose tissues were digested with 1 mg/mL Type I collagenase at 37 °C for 30 min and then filtered using the 40-μm cell strainer. After centrifugation at 200*g* for 5 min, the cell pellets were incubated in erythrocyte lysis buffer for 10 min at 4 °C, followed by centrifugation at 200*g* for 5 min. The isolated ADSCs were cultured in DMEM/F-12 (Thermo Fisher) supplemented with 10% FBS (Gibco, USA).

To evaluate the multidirectional differentiation capacities, ADSCs were maintained in adipogenic (Gibco) or osteogenic (Gibco) differentiation media for 3 weeks with medium changed every 2 days. Then, differentiated ADSCs were subjected to Oil Red O staining (Sigma-Aldrich, USA), and Alizarin Red S staining (Sigma-Aldrich) to verify adipogenic and osteogenic differentiation, respectively.

2.9. Isolation and characterization of ADSCs-derived EVs

To isolate EVs, ADSCs with 80% confluence were cultured in 10% exosome-depleted FBS (Thermo Fisher) for 48 h. Subsequently, the supernatant was collected and dead cells and cellular debris were removed by differential centrifugation at 300*g* for 10 min, at 2000 g for 10 min, and subsequent filtration through a 0.22 μm filter. Then, the EVs were collected by centrifugation at 10,000 g for 30 min, followed by ultracentrifugation at 178,000 g for 2 h. After the centrifugation, the pellets were resuspended in sterile PBS. ADSCs-derived EVs were examined using the transmission electron microscope (TEM) to observe their morphology. Size distribution of ADSCs-derived EVs was evaluated by nanoparticle tracking analysis (Nanosight NS300, Malvern, UK). In addition, the levels of biomarkers for EVs, including TSG101 and CD63, and endoplasmic reticulum biomarker, Calnexin were assessed by Western blotting.

2.10. Uptake of ADSC-EVs by MAECs

The ADSCs-derived EVs were labeled with PKH26 (Sigma-Aldrich) following the provided protocol. Then, MAECs were incubated with PKH26-labeled EVs at 37 °C for 4 h. After fixation with 4% paraformaldehyde, the MAECs were counterstained with DAPI. The uptake of ADSC-EVs was observed under a fluorescence microscope.

2.11. Cell transfection

Lentivirus carrying antagomir-miR-674-5p (*anti*-miR-674-5p) or antagomir NC (scramble), shRNA targeting CTRP9 (sh-CTRP9) or sh-NC, CTRP9 overexpression plasmid or vector were packaged by GenePharma. MAECs or ADSCs were infected with the produced recombinant lentivirus supplemented with 8 mg/mL Polybrene.

2.12. Cell counting kit-8 (CCK-8)

To evaluate cell viability, MAECs were planted into 96-well plates (3000 cells per well). After various treatments, MAECs were reacted with 10 μL of CCK-8 reagent (Solarbio) at 37 °C for 2 h. The results were detected at 450 nm on a microplate reader (Thermo Fisher).

2.13. 5-Ethynyl-2′-deoxyuridine (EdU) assay

The iClick™ EdU Andy Fluor 594 Imaging Kit (GeneCopoeia, Guangzhou, China) was adopted to monitor ADSCs proliferation. Briefly, ADSCs were labeled with 10 μM EdU solution for 2 h. The labeled ADSCs were fixed with 3.7% formaldehyde and infiltrated with 0.5% Triton X-100 for 20 min. The cells were stained with iClick reaction buffer, and counterstained with DAPI (Beyotime). Under a fluorescence microscope, the stained ADSCs were observed and photographed. The percentage of EdU positive cells was quantified using Image J software.

2.14. Determination of lactate dehydrogenase (LDH), lipid peroxide (LPO), and malondialdehyde (MDA)

The levels of LDH, LPO, and MDA in MAECs were measured using the commercial LDH Activity Assay Kit (Solarbio), LPO Content Assay Kit (Solarbio), MDA Content Assay Kit (Solarbio), according to the provided protocols, respectively.

2.15. Flow cytometry

Annexin V-FITC/PI staining was conducted to detect apoptosis of MAECs. After digestion, MAECs with various treatments were resuspended in labeling solution, followed by adding with Annexin V-FITC (5 μL) and PI solution (5 μL). After staining for 20 min in dark, the MAECs were analyzed on a flow cytometer (Agilent, USA).

2.16. Detection of reactive oxygen species (ROS)

For total ROS measurement, MAECs with indicated treatments were added with 10 μmol/L DCFH-DA (Solarbio) and incubated at 37 °C for 20 min. For lipid ROS detection, MAECs from different groups were stained with 50 μM C11-BODIPY (Thermo Fisher) for 1 h. Redundant DCFH-DA or C11-BODIPY was eliminated by rinsing with PBS for three times. The labeled MAECs were analyzed on a microplate reader.

2.17. Transwell assay

The treated MAECs or ADSCs were resuspended in serum-free medium. A 200 μL cell suspension containing 5×10^4 cells was added into the top Transwell chambers (Corning, USA), while 500 μL culture medium containing 10% FBS was added into the bottom chambers. After culture for 24 h, MAECs or ADSCs traversing the membranes were stained with 0.1% crystal violet for 15 min and photographed under a light microscope.

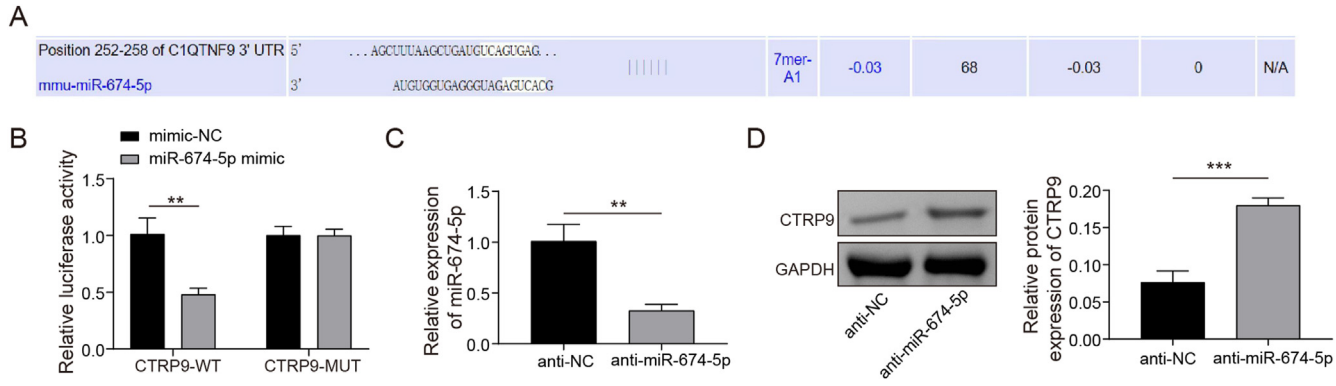

Fig. 1. CTRP9 was a target gene of miR-674-5p. (A) The potential binding sites of miR-674-5p to CTRP9 3′UTR were predicted by miRDB database. (B) The direct binding between miR-674-5p and CTRP9 was validated by dual luciferase reporter assay. MAECs were infected with lentivirus carrying antagomir-miR-674-5p or antagomir NC. (C) qRT-PCR analysis of miR-674-5p expression in MAECs. (D) Protein abundance of CTRP9 in MAECs was determined by Western blotting. Values were shown as mean ± SD (n = 3). **p < 0.01, ***p < 0.001.

2.18. Tube formation assay

To evaluate tube formation, the 96-well plates were pre-coated with Matrigel (BD Falcon, USA). Subsequently, 1.5 × 10^4 MAECs were seeded into 96-well plates. After incubation at 37 °C for 24 h, the capillary-like structure formation was observed and photographed using a light microscopy. The tube length and branch points were analyzed using the AxioVision Rel (Carl Zeiss AG, Germany) software.

2.19. Animals and treatment

Male *ApoE*$^{-/-}$ (C57BL/6J background, six weeks old) mice and age-matched male wild type C57BL/6 J mice were provided by Shanghai Biomodel Organism. To establish AS model, *ApoE*$^{-/-}$ mice were fed with high-fat diet (HFD, Research Diets, USA) for 16 weeks. C57BL/6J mice were fed with normal diet. At 8 weeks after HFD feeding, the AS model mice were divided into 2 groups: 1) model group, 200 μl of PBS was injected into the mice via tail vein once a

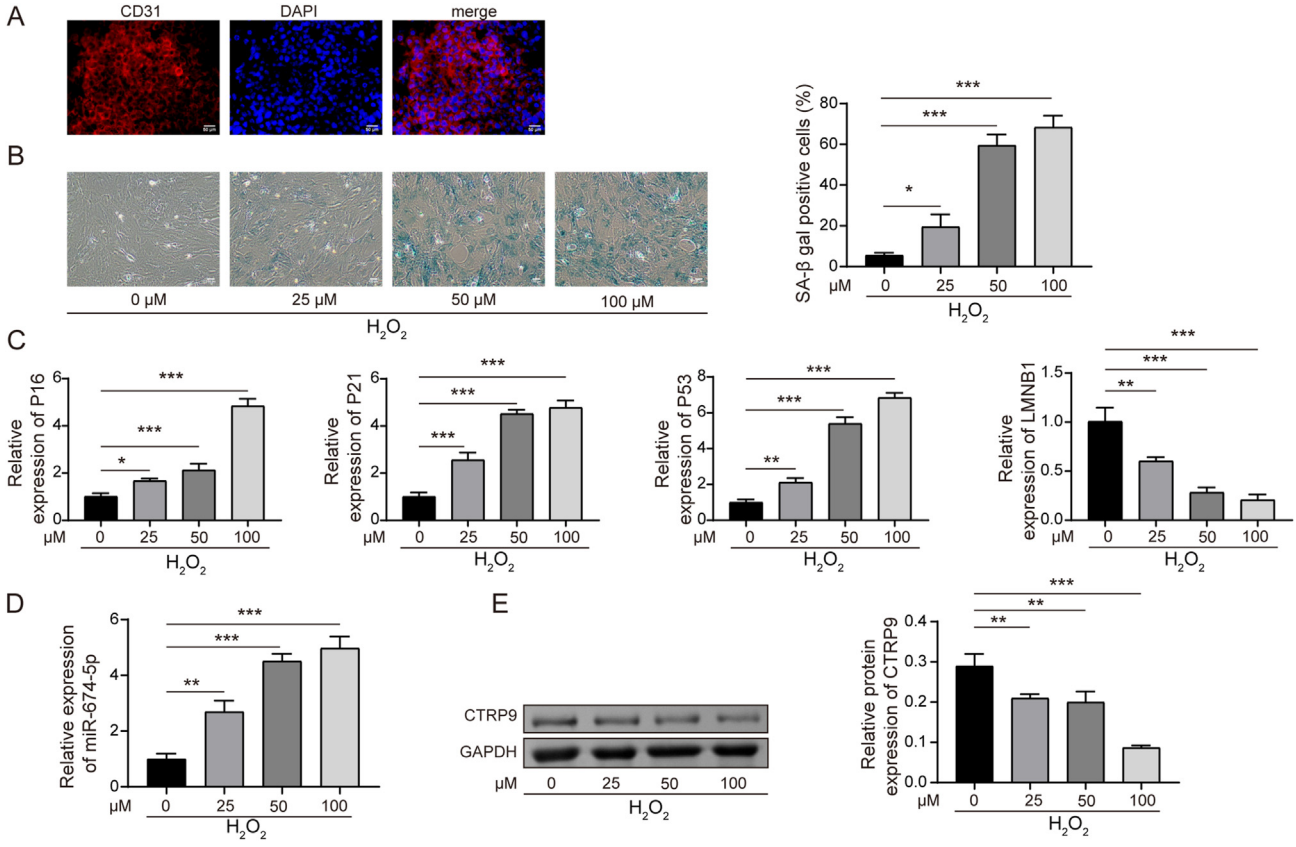

Fig. 2. miR-674-5p was up-regulated and CTRP9 was down-regulated in H_2O_2-induced senescence of MAECs. (A) Identification of MAECs by immunofluorescent staining of CD31. MAECs were exposed to H_2O_2 (0, 25, 50, 100 μM) for 24 h. (B) Senescence of MAECs was evaluated by SA-β-gal staining. (C) qRT-PCR analysis of mRNA levels of senescence markers P16, P21, P53, and LMNB1. (D) miR-674-5p expression in MAECs was detected by qRT-PCR. (E) Western blotting analysis of CTRP9 expression in MAECs. Values were shown as mean ± SD (n = 3). *p < 0.05, **p < 0.01, ***p < 0.001.

day for 8 weeks; 2) ADSC-EVs + *Anti*-miR-674-5p group, 200 μl of ADSC-EVs (0.5 mg/mL) combined with antagomir-miR-674-5p (100 μg) was injected into the mice via tail vein once a day for 8 weeks. HFD feeding was maintained for another 8 weeks during injection. At the end of the experiments, serum samples were obtained and all mice were euthanized by cervical dislocation.

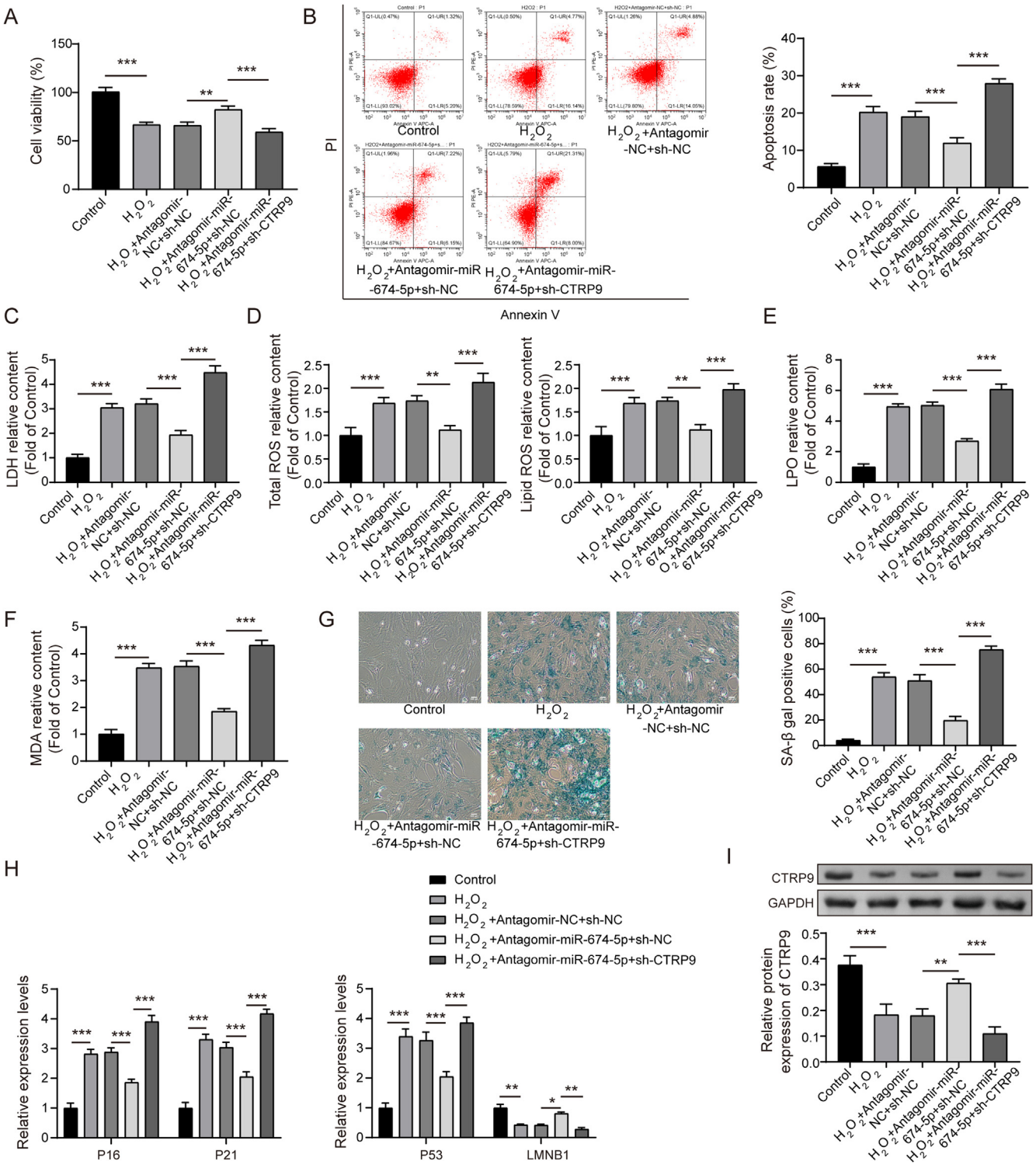

Fig. 3. miR-674-5p inhibition repressed H_2O_2-induced senescence of MAECs via target regulation of CTRP9. MAECs were infected with lentivirus containing Antagomir-miR-674 combined with or without sh-CTRP9, followed by stimulation with H_2O_2. (A) Cell viability was measured by CCK-8 assay. (B) Apoptosis of MAECs was evaluated by flow cytometry. (C–F) The levels of LDH, total ROS, lipid ROS, LPO, and MDA in MAECs were determined by commercial kits. (G) Senescence of MAECs was assessed by SA-β-gal staining. (H) P16, P21, P53, and LMNB1 mRNA levels were detected by qRT-PCR. (I) The protein abundance of CTRP9 was measured by Western blotting. Values were shown as mean ± SD (n = 3). *p < 0.05, **p < 0.01, ***p < 0.001.

2.20. Serum lipid analysis

The mouse serum levels of triglycerides (TG), total cholesterol (TC), and low-density lipoprotein (LDL-C) were detected using the automatic biochemical analyzer (Hitachi, Japan).

2.21. Histological examination

The arteries of the mice were collected and fixed in 10% neutral buffered formalin. To determine atherosclerotic lesions, the arteries were embedded in optimal cutting temperature compound, and sliced into 8-μm sections. The sections were subjected to hematoxylin-eosin (HE) staining and Masson's staining using the HE Stain Kit (Solarbio) and the Masson's Trichrome Stain Kit (Solarbio) and quantitively analyzed using the Image J software.

2.22. Statistical analysis

Data are expressed as the mean ± standard deviation (SD) from at least three independent experiments. Statistical significances were evaluated by Student's t-test for two groups, and a one-way analysis of variance with Tukey's post-hoc test for multiple groups using SPSS 22.0. $p < 0.05$ was defined as statistical significance.

3. Results

3.1. CTRP9 was identified as a target of miR-674-5p

As predicted by miRDB and Targetscan databases, miR-674-5p is the only candidate that possesses binding sites on CTRP9 3′-untranslated regions (UTR) by overlapping the results (Fig. 1A). Thus, miR-674-5p was focused on. Furthermore, the luciferase activity of CTRP9 WT was evidently lowered by miR-674-5p mimic, while that of CTRP9 MUT was not changed, suggesting the direct interplay between miR-674-5p and CTRP9 (Fig. 1B). To validate the modulation of miR-674-5p in CTRP9 expression, MAECs were infected with lentivirus carrying antagomir-miR-674-5p. Lentivirus-mediated down-regulation of miR-674-5p in MAECs was verified by qRT-PCR assay (Fig. 1C). Notably, the protein level of CTRP9 in miR-674-5p-down-regulated MAECs was remarkably elevated (Fig. 1D). Therefore, CTRP9 was demonstrated as a target gene of miR-674-5p.

3.2. Abnormal up-regulation of miR-674-5p and down-regulation of CTRP9 in H_2O_2-induced senescence of MAECs

Next, a senescent cell model was established through H_2O_2 exposure in primary MAECs. As illustrated in Fig. 2A, the primary MAECs were identified by positive expression of CD31 via immunofluorescence staining. Subsequently, we evaluated the senescence of MAECs using SA-β-gal staining, and found that the percentage of senescent MAECs was dose dependently enhanced by H_2O_2 (Fig. 2B). Moreover, the senescence markers P16, P21, and P53 were up-regulated, but LMNB1 was down-regulated in MAECs with the increasing of H_2O_2 concentration (Fig. 2C). Additionally, we observed an increase in miR-674-5p expression, while a reduction in CTRP9 expression after H_2O_2 challenge in a dose dependent manner (Fig. 2DandE). These data indicated that miR-674-5p was up-regulated and CTRP9 was down-regulated during H_2O_2-induced senescence in MAECs.

As the therapeutic action of CTRP9 on AS has been documented, subsequently, we performed rescue experiments to investigate whether overexpression of CTRP9 could rescue senescence phenotypes in H_2O_2-treated model. We found that the decreased expression of CTRP9 in H_2O_2-treated MAECs was restored by infection with lentiviruses containing CTRP9 overexpression plasmid (Fig. S1A). In addition, CTRP9 overexpression partly weakened the enhanced percentage of SA-β-gal positive cells after H_2O_2 exposure (Fig. S1B). Besides, H_2O_2-mediated up-regulation of P16, P21, and P53, and down-regulation of LMNB1 were partially reversed by CTRP9 overexpression (Fig. S1C).

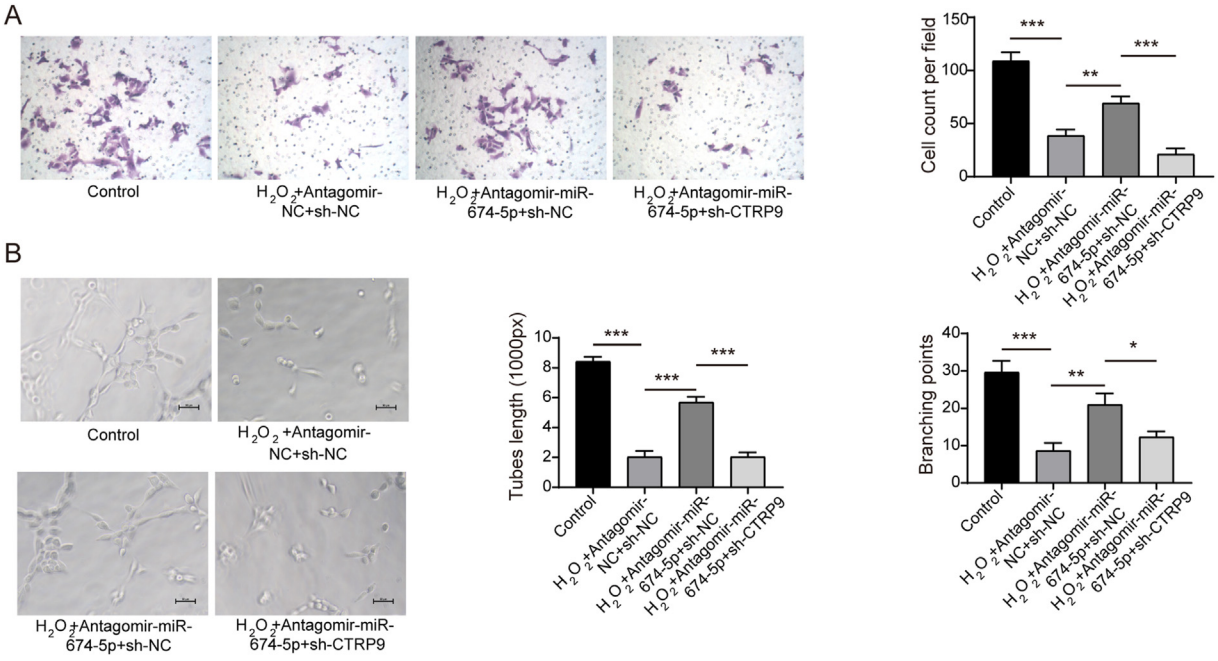

Fig. 4. miR-674-5p down-regulation restored the impaired migration and angiogenesis of H_2O_2-treated MAECs via up-regulation of CTRP9. Lentivirus containing Antagomir-miR-674 combined with or without sh-CTRP9 were infected into H_2O_2-exposed MAECs. (A) The migratory ability of MAECs was determined by Transwell assay. (B) The angiogenesis of MAECs was evaluated by tube formation assay. Values were shown as mean ± SD (n = 3). *p < 0.05, **p < 0.01, ***p < 0.001.

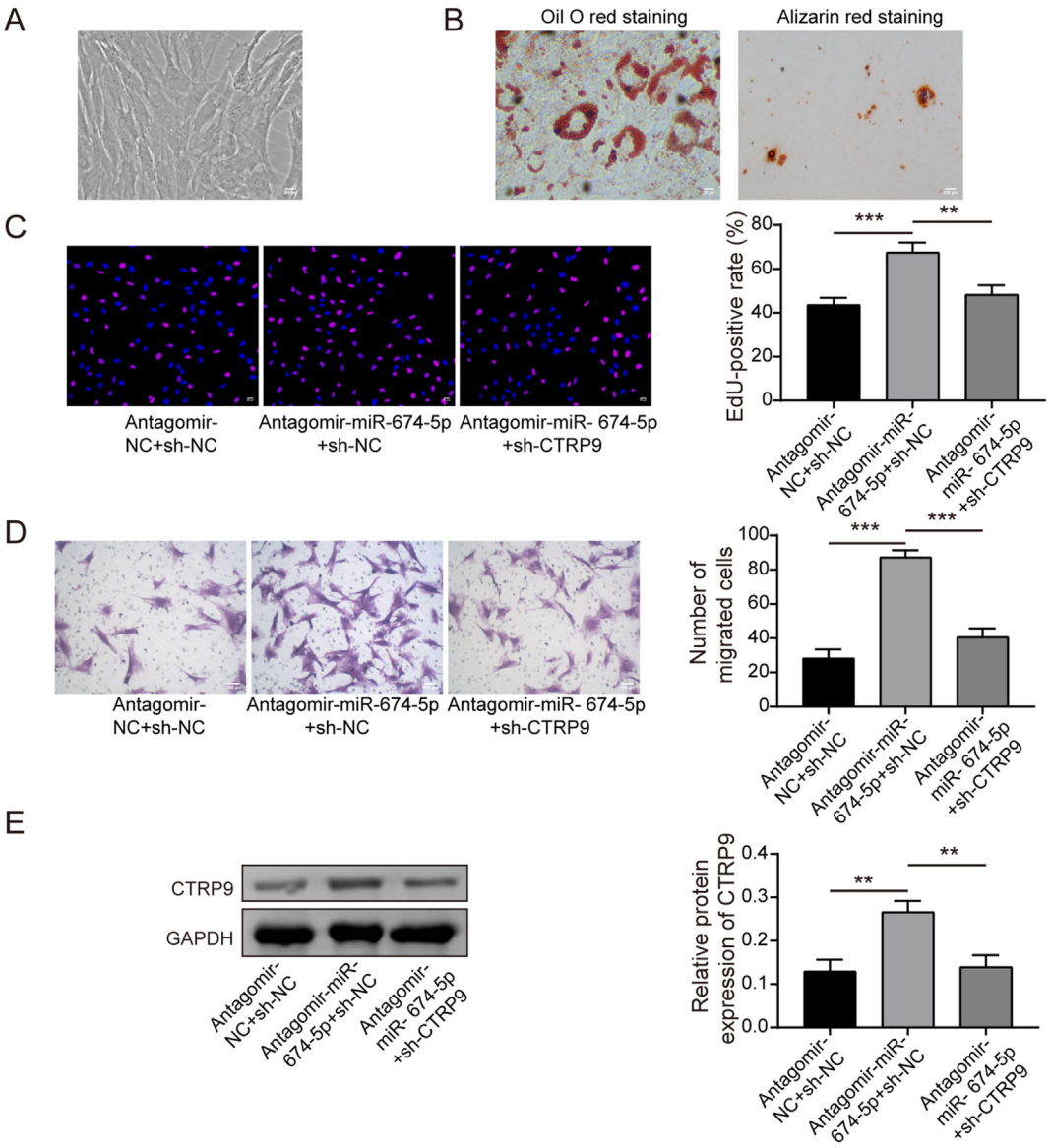

Fig. 5. miR-674-5p silencing contributed to proliferation and migration of ADSCs through enhancing CTRP9 expression. (A) The morphology of ADSCs was observed under an optical microscope (200 ×). (B) Oil red O staining and Alizarin red staining were performed to evaluate the adipogenic and osteogenic differentiation abilities of ADSCs (200 ×). (C) EdU assay for the detection of cell proliferation of ADSCs. (D) The migration of ADSCs was detected by Transwell assay. (E) Western blotting analysis of CTRP9 protein abundance in ADSCs. Values were shown as mean ± SD (n = 3). **p < 0.01, ***p < 0.001.

3.3. Down-regulation of miR-674-5p targeted CTRP9 to mitigate H_2O_2-induced impaired viability and senescence of MAECs

Given that miR-674-5p/CTRP9 axis was dysregulated during MAEC senescence, we further explored its biological functions. For this purpose, MAECs were infected with lentiviruses containing antagomir-miR-674-5p together with or without sh-CTRP9. The viability of MAECs was strikingly reduced by H_2O_2 stimulation, which was partly elevated by miR-674-5p silencing. However, antagomir-miR-674-5p-mediated improvement in MAEC viability was abolished by CTRP9 knockdown (Fig. 3A). Besides, H_2O_2 exposure-triggered apoptosis of MAECs was restrained by miR-674-5p inhibition, whereas CTRP9 depletion reversed the inhibitory effect of antagomir-miR-674-5p (Fig. 3B). Furthermore, the enhanced levels of LDH, total ROS, lipid ROS, LPO, and MDA in H_2O_2-stimulated MAECs were decreased after miR-674-5p down-regulation, which could be counteracted by CTRP9 deficiency (Fig. 3C–F). Additionally, miR-674-5p silencing strikingly decreased the percentage of senescent MAECs induced by H_2O_2, however; CTRP9 depletion remarkably elevated senescent MAEC proportion (Fig. 3G). Accordingly, antagomir-miR-674-5p down-regulated P16, P21, and P53, while up-regulated LMNB1 in H_2O_2-exposed MAECs, which were reversed by CTRP9 silencing (Fig. 3H). As assessed by Western blotting, the decreased CTRP9 protein level in H_2O_2-challenged MAECs was prominently raised by antagomir-miR-674-5p, whereas sh-CTRP9 abrogated the promotive effect of antagomir-miR-674-5p (Fig. 3I). Collectively, down-regulation of miR-674-5p enhanced CTRP9 expression to protect against H_2O_2-induced impaired viability and senescence of MAECs.

3.4. miR-674-5p inhibition repressed H_2O_2-induced impaired migration and angiogenesis of MAECs via regulating CTRP9

To further investigate the migrative capacity of MAECs, transwell assay was conducted. H_2O_2 stimulation distinctly suppressed

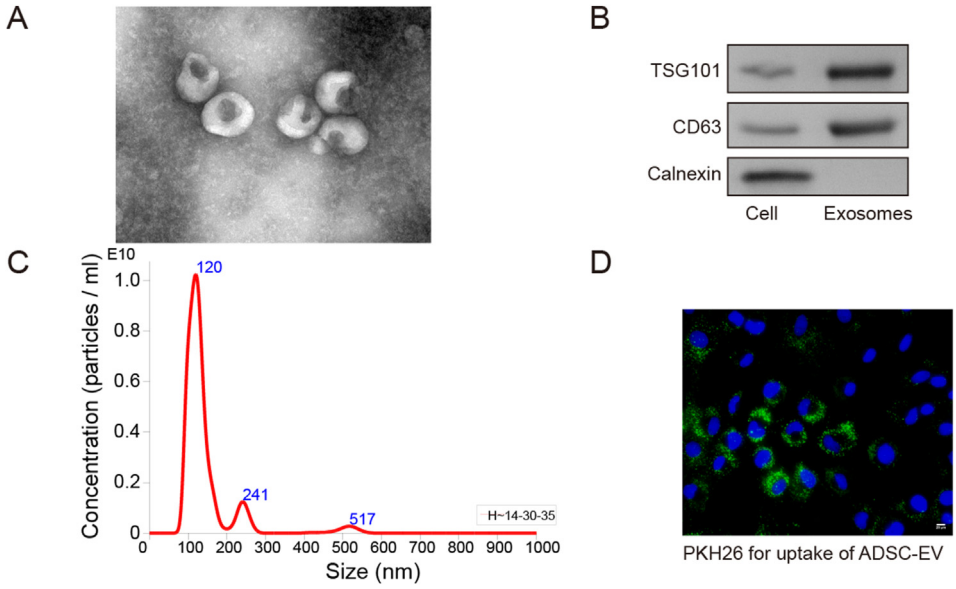

Fig. 6. Identification of ADSC-EVs and their internalization by MAECs. (A) ADSC-EVs were examined under a transmission electron microscope (TEM). (B) The protein levels of TSG101, CD63, and Calnexin in ADSC and ADSC-EVs were detected by Western blotting. (C) The particle distribution of ADSC-EVs was evaluated by nanoparticles tracking analysis. (D) Uptake of PKH26-labeled ADSC-EVs by MAECs was observed under a fluorescence microscope. Values were shown as mean ± SD (n = 3).

migration of MAECs, which was greatly recovered by miR-674-5p inhibition. However, antagomir-miR-674-5p-mediated migration of MAECs was abolished after CTRP9 was depleted (Fig. 4A). Furthermore, tube formation assay indicated that the angiogenic ability of MAECs was impaired by H_2O_2 challenge. miR-674-5p down-regulation effectively improved the angiogenesis of MAECs upon H_2O_2 exposure, which was counteracted in CTRP9-deficient MAECs (Fig. 4B). Therefore, miR-674-5p silencing restored the migration and angiogenesis of H_2O_2-induced MAECs via the regulation of CTRP9.

3.5. Down-regulation of miR-674-5p promoted proliferation and migration of ADSCs through increasing CTRP9 expression

Transplantation of ADSCs has been shown to alleviate AS through suppressing endothelial dysfunction [22]. Thus, we further evaluated the biological function of miR-674-5p/CTRP9 axis in ADSCs. The primary ADSCs were isolated from C57BL/6J mice and their morphology was observed under a light microscope (Fig. 5A). The adipogenic and osteogenic differentiation capacities of ADSCs were confirmed by Oil red O and Alizarin red staining (Fig. 5B). Subsequently, lentivirus carrying antagomir-miR-674-5p combined with sh-CTRP9 or sh-NC were infected into ADSCs. EdU assay suggested that the proliferation of ADSCs was facilitated by miR-674-5p inhibition, whereas CTRP9 down-regulation reversed antagomir-miR-674-5p-meidated enhancement in proliferation (Fig. 5C). Moreover, antagomir-miR-674-5p enhanced the migrative ability of ADSCs, which was counteracted by CTRP9 knockdown (Fig. 5D). Western blotting indicated that miR-674-5p silencing remarkably increased CTRP9 expression in ADSCs, however, sh-CTRP9 deliver evidently reversed up-regulation of CTRP9 (Fig. 5E). The above findings revealed that miR-674-5p silencing facilitated the proliferative and migrative abilities of ADSCs via up-regulating CTRP9.

3.6. Characterization of ADSC-EVs and their internalization by MAECs

It has been identified that ADSCs exert their function predominantly via delivering information to recipient cells through releasing EVs [23]. Therefore, we extracted EVs from ADSCs. The round or cup-shaped morphology of ADSC-EVs was found using TEM (Fig. 6A). In addition, we validated the presence of biomarkers of EVs TSG101 and CD63, and absence of endoplasmic reticulum biomarker Calnexin in ADSC-EVs (Fig. 6B). Nanoparticles tracking analysis revealed that the particle size distribution of ADSC-EVs was 50–200 nm (Fig. 6C). Moreover, the internalization of PKH26-labeled ADSC-EVs by MAECs was observed under a fluorescence microscope (Fig. 6D). These observations indicated that ADSC-EVs were successfully isolated and could be internalized by MAECs.

3.7. ADSC-EVs rescued the impaired biological functions and senescence of H_2O_2-triggered MAECs

We further investigated the therapeutic efficacy of ADSC-EVs on H_2O_2-triggered dysfunction in MAECs. The decreased viability of MAECs upon H_2O_2 exposure was restored by administration with ADSC-EVs (Fig. 7A). Besides, treatment with ADSC-EVs reversed the elevated levels of LDH, total ROS, lipid ROS, LPO, and MDA in H_2O_2-stimulated MAECs (Fig. 7B–E). Moreover, the senescent MAEC percentage was lowered by ADSC-EVs (Fig. 7F). In addition, ADSC-EVs led to down-regulation of P16, P21, and P53, and up-regulation of LMNB1 in H_2O_2-treated MAECs (Fig. 7G). The impaired migration and angiogenesis induced by H_2O_2 was improved after intervention with ADSC-EVs (Fig. 7H and I). Notably, we observed a reduction in miR-674-5p expression, and increase in CTRP9 expression in ADSC-EVs-treated MAECs (Fig. 7J and K). To sum up, H_2O_2-induced dysfunction and senescence of MAECs were attenuated by ADSC-EVs.

3.8. ADSC-EVs combined with anti-miR-674-5p attenuated AS development in $ApoE^{-/-}$ mice

Finally, the influence of ADSCs EVs in combination with *anti*-miR-674-5p on AS progression *in vivo* was explored. The enhanced TC, TG, and LDL-C levels of AS mice were effectively reduced by *anti*-miR-674-5p combined with ADSC-EVs (Fig. 8A–C). Histological examination showed that the atherosclerotic lesion area and

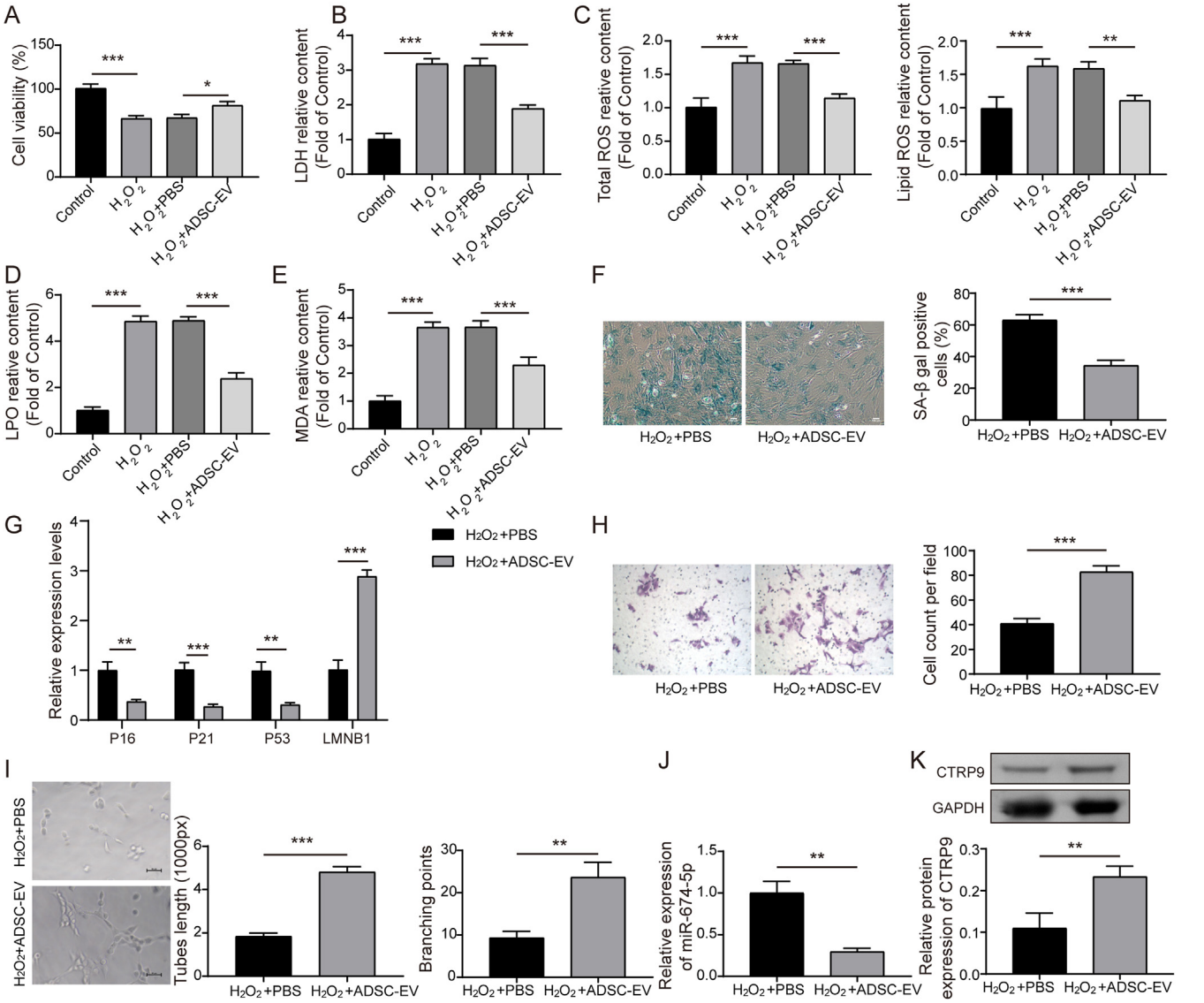

Fig. 7. ADSC-EVs suppressed H_2O_2-induced dysfunction and senescence of MAECs. H_2O_2-exposed MAECs were treated with ADSC-EVs or PBS. (A) Cell viability of MAECs was detected by CCK-8. (B–E) The levels of LDH, total ROS, lipid ROS, LPO, and MDA in MAECs were measured by commercial kits. (F) Senescent MAECs were assessed by SA-β-gal staining. (G) P16, P21, P53, and LMNB1 mRNA levels were determined by qRT-PCR. (H) The migratory ability of MAECs was evaluated by Transwell assay. (I) The angiogenesis of MAECs was detected by tube formation assay. (J) qRT-PCR analysis of miR-674-5p expression in MAECs. (K) The protein abundance of CTRP9 was measured by Western blotting. Values were shown as mean ± SD (n = 3). *p < 0.05, **p < 0.01, ***p < 0.001.

collagen deposition area were strikingly raised in the arteries of model group, which were weakened by *anti*-miR-674-5p plus ADSC-EVs (Fig. 8D and E). Accordingly, miR-674-5p was up-regulated, while CTRP9 was down-regulated in the arteries of AS mice, which were reversed by ADSC-EVs together with miR-674-5p inhibition (Fig. 8F and G). Taken together, the progression of AS in mice was delayed by ADSC-EVs combined with *anti*-miR-674-5p via promoting CTRP9 expression.

4. Discussion

AS remains a chronic vascular disorder, which is closely associated with aging. The senescence of vascular endothelial cells may result in inflammatory response and oxidative damage and causes endothelial dysfunction, thereby promoting the progression of AS [24]. Therefore, uncovering the modulatory mechanisms of endothelial cell senescence is vital to develop effective therapies for delaying AS development. In this paper, we provided first evidence that miR-674-5p inhibition attenuated H_2O_2-induced senescence in MAECs by enhancing CTRP9 expression. In addition, ADSC-EVs conferred protection against endothelial senescence and dysfunction through modulation of miR-674-5p/CTRP9 pathway. More importantly, the combination of ADSC-EVs with *anti*-miR-674-5p repressed atherosclerotic plaque formation *in vivo*. Our findings provide theoretical basis for the development of effective therapy for treating endothelial cell senescence during AS.

As an endogenous cardiovascular protector, CTRP9 is responsible for vascular relaxation [25]. Down-regulation of CTRP9 has been found in obese mice [26]. CTRP9 was reported to enhance carotid plaque stability by restraining macrophage inflammation [27]. Extensive evidence has suggested that CTRP9 exerted protection against endothelial dysfunction and maintained vascular homeostasis [28,29]. It has been documented that CTRP9 restrained endothelial cell senescence to mitigate diabetic-associated AS [9]. Therefore, targeting CTRP9 has been recognized as a therapeutic strategy for AS. However, the upstream modulatory mechanism of

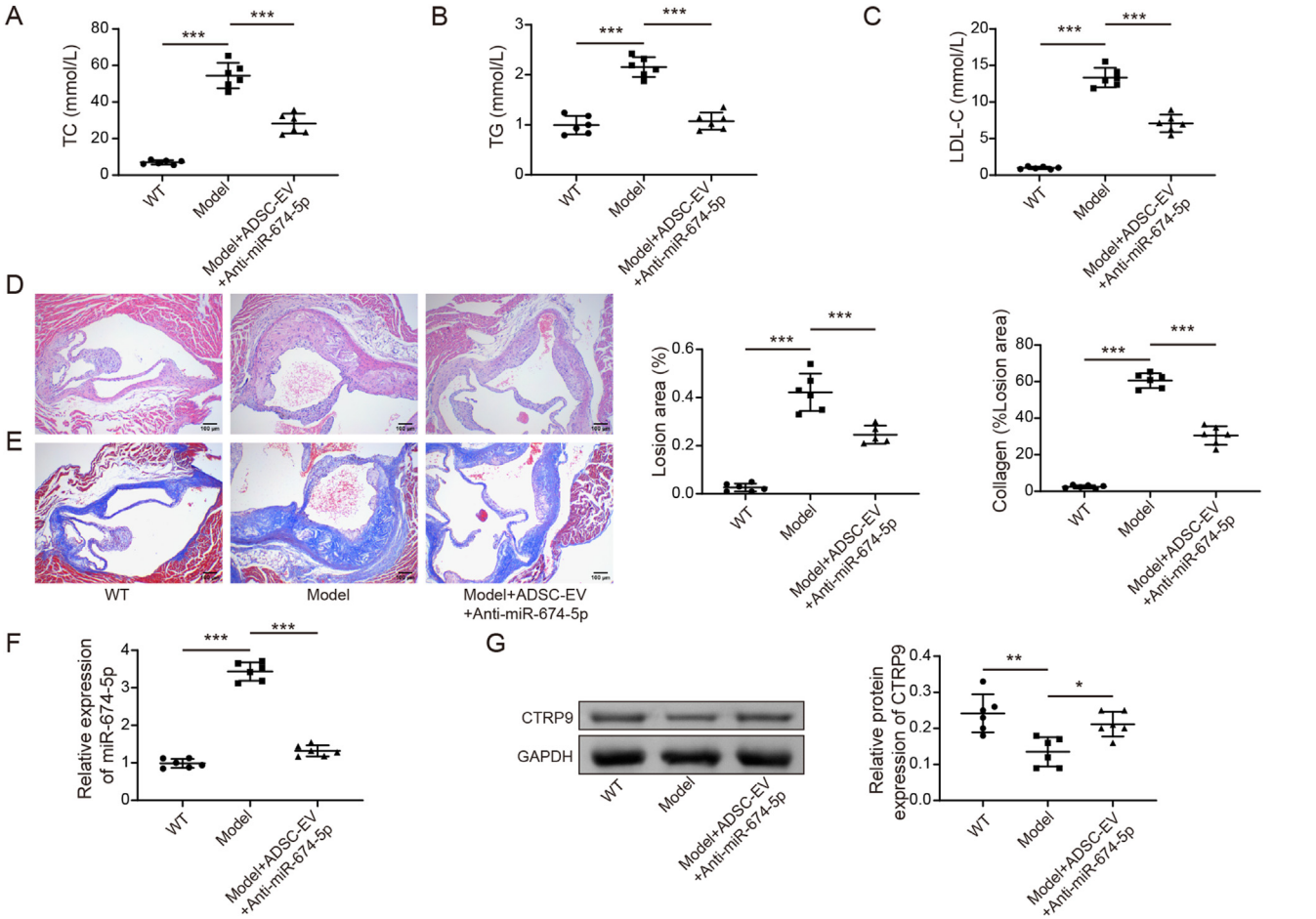

Fig. 8. ADSC-EVs-*anti*-miR-674-5p combined treatment delayed AS development in $ApoE^{-/-}$ mice. $ApoE^{-/-}$ mice were injected with PBS or ADSC-EVs + *Anti*-miR-674-5p after 8 weeks of HFD via caudal vein, followed by HFD feeding for another 8 weeks. (A–C) TC, TG, and LDL-C levels were detected. (D) Atherosclerotic lesions in the aortic sinus were observed by HE staining. (E) Collagen deposition in the aortic sinus was evaluated by Masson staining. (F) qRT-PCR analysis of miR-674-5p expression in the arteries. (G) The protein abundance of CTRP9 was analyzed by Western blotting. Data are reported as mean ± SD (n = 6). *p < 0.05, **p < 0.01, ***p < 0.001.

CTRP9 in AS remains largely unknown. MicroRNAs (miRNAs) can negatively modulate target gene expression via directly binding to the 3′-UTR to prevent protein translation [30]. miRNAs have been revealed to exert pivotal roles in diverse diseases, including AS. For instance, down-regulation of miR-98 drove AS progression via inducing endothelial cell dysfunction [31]. In this work, we identified that miR-674-5p was aberrantly highly expressed in senescent MAECs, and predicted miR-674-5p as a potential candidate for binding to CTRP9. miR-674-5p is located on mouse genome GRCm38. So far, the regulation of miR-674-5p in AS has not been documented. For the first time, we demonstrated that miR-674-5p inhibition restrained endothelial cell senescence and dysfunction via up-regulating CTRP9. Therefore, miR-674-5p selectively targeted CTRP9 in H2O2-induced endothelial cell senescence during AS.

MSCs with tissue repair capacities have been used for treating AS [4]. However, the clinical application of MSCs has been constrained by the lower survival of transplanted MSCs, vascular thrombosis, and immune rejection [32]. EVs derived from MSCs can solve the above problems and are recognized as a perfect alternative to MSCs MSC therapies [33]. Previous studies have suggested BMSC-derived EVs as an effective therapy to attenuate AS symptoms [4,34]. A previous study suggested that BMSC-derived EVs repressed endothelial dysfunction during the progression of AS in hamsters [35]. In this study, ADSC-EVs had a protective action against AS via up-regulating CTRP9 and down-regulating miR-674-5p, thereby reducing endothelial senescence and improving the biological functions of MAECs. Our study elucidated a novel mechanism by which ADSC-EVs mitigated endothelial senescence in AS. Other potential miRNAs might also affect endothelial cell senescence via targeting CTRP9, which is considered as a limitation of this study. In our future study, we will investigate the biological functions of other potential miRNAs during this process.

5. Conclusions

In conclusion, this study proved that ADSC-EVs relieved AS by suppressing endothelial senescence. ADSC-EVs-mediated promotion of CTRP9 expression may be key to attenuate endothelial senescence in AS, which was intensified by miR-674-5p inhibition. Our observations shed light on the mechanisms underlying ADSC-EVs-mediated beneficial actions on AS, and provide theoretical foundation for its clinical application in treating AS.

Ethics approval and consent to participate

The animal procedures were conducted in compliance with the Directive 2010/63/EU of the European Parliament on animal protection and approved by the Ethic Committee of Hainan Affiliated Hospital of Hainan Medical University (Hainan General Hospital).

Consent for publication

Not applicable.

Availability of data and materials

All data generated or analyzed are included in this article. Further inquiries can be directed to the corresponding author.

Funding

This work was supported by Hainan Clinical Medical Research Center Project (LCYX202207 and LCYX202305), Hainan General Hospital Clinical Innovation and Transformation Cultivation 550 Project (2022CXZH01) and Hainan Provincial Health Industry Research Project (22A200216).

Authors' contributions

Min Zeng and Yangli He conceived and designed the research. Yangli He, Yali Yang and Mengdi Wang performed the research and acquired the data. Yue Chen, Xin Wei and Min Zeng analyzed and interpreted the data. All authors were involved in drafting and revising the manuscript.

Declaration of competing interest

The authors declare that they have no known competing financial interests or personal relationships that could have appeared to influence the work reported in this paper.

Acknowledgements

We would like to give our sincere gratitude to the reviewers for their constructive comments.

Appendix A. Supplementary data

Supplementary data to this article can be found online at https://doi.org/10.1016/j.reth.2024.03.027.

References

[1] Libby P, Buring JE, Badimon L. Atherosclerosis. Nat Rev Dis Prim 2019;5:56.
[2] Li TT, Wang ZB, Li Y. The mechanisms of traditional Chinese medicine underlying the prevention and treatment of atherosclerosis. Chin J Nat Med 2019;17:401–12.
[3] Zarzycka B, Nicolaes GA, Lutgens E. Targeting the adaptive immune system: new strategies in the treatment of atherosclerosis. Expet Rev Clin Pharmacol 2015;8:297–313.
[4] Sun L, He X, Zhang T. Knockdown of mesenchymal stem cell-derived exosomal LOC100129516 suppresses the symptoms of atherosclerosis via upregulation of the PPARgamma/LXRalpha/ABCA1 signaling pathway. Int J Mol Med 2021;48.
[5] Tunon J, Badimon L, Bochaton-Piallat ML. Identifying the anti-inflammatory response to lipid lowering therapy: a position paper from the working group on atherosclerosis and vascular biology of the European Society of Cardiology. Cardiovasc Res 2019;115:10–9.
[6] Kruger-Genge A, Blocki A, Franke RP. Vascular endothelial cell biology: an update. Int J Mol Sci 2019;20.
[7] Higashi Y, Kihara Y, Noma K. Endothelial dysfunction and hypertension in aging. Hypertens Res 2012;35:1039–47.
[8] Minamino T, Komuro I. Vascular cell senescence: contribution to atherosclerosis. Circ Res 2007;100:15–26.
[9] Wang G, Han B, Zhang R. C1q/TNF-Related protein 9 attenuates atherosclerosis by inhibiting hyperglycemia-induced endothelial cell senescence through the AMPKalpha/KLF4 signaling pathway. Front Pharmacol 2021;12:758792.
[10] Song CX, Chen JY, Li N. CTRP9 enhances efferocytosis in macrophages via MAPK/Drp1-Mediated mitochondrial fission and AdipoR1-induced immunometabolism. J Inflamm Res 2021;14:1007–17.
[11] Zuo A, Zhao X, Li T. CTRP9 knockout exaggerates lipotoxicity in cardiac myocytes and high-fat diet-induced cardiac hypertrophy through inhibiting the LKB1/AMPK pathway. J Cell Mol Med 2020;24:2635–47.
[12] Na N, Ji M. Role of first-trimester serum C1q/TNF-related protein 9 in gestational diabetes mellitus. Clin Lab 2020;66.
[13] Wang G, Han B, Zhang R. Corrigendum: C1q/TNF-related protein 9 attenuates atherosclerosis by inhibiting hyperglycemia-induced endothelial cell senescence through the AMPKalpha/KLF4 signaling pathway. Front Pharmacol 2021;12:812384.
[14] Zeng M, Wei X, He Y. Ubiquitin-specific protease 11-mediated CD36 deubiquitination acts on C1q/TNF-related protein 9 against atherosclerosis. ESC Heart Fail 2023;10:2499–509.
[15] Zhang H, Gong X, Ni S. C1q/TNF-related protein-9 attenuates atherosclerosis through AMPK-NLRP3 inflammasome singling pathway. Int Immunopharm 2019;77:105934.
[16] Yang S, Xiao X, Huang Z. Human adipose-derived mesenchymal stem cell-based microspheres ameliorate atherosclerosis progression in vitro. Stem Cell Dev 2023;32:314–30.
[17] Casado-Diaz A, Quesada-Gomez JM, Dorado G. Extracellular vesicles derived from mesenchymal stem cells (MSC) in regenerative medicine: applications in skin wound healing. Front Bioeng Biotechnol 2020;8:146.
[18] Li T, Wang B, Ding H. Effect of extracellular vesicles from multiple cells on vascular smooth muscle cells in atherosclerosis. Front Pharmacol 2022;13:857331.
[19] Yu XH, Zhang DW, Zheng XL. C1q tumor necrosis factor-related protein 9 in atherosclerosis: mechanistic insights and therapeutic potential. Atherosclerosis 2018;276:109–16.
[20] Wang JM, Chen AF, Zhang K. Isolation and primary culture of mouse aortic endothelial cells. J Vis Exp 2016;118:52965.
[21] Saito T, Kotani T, Suzuka T. Adipose-derived stem/stromal cells with heparin-enhanced anti-inflammatory and antifibrotic effects mitigate induced pulmonary fibrosis in mice. Biochem Biophys Res Commun 2022;629:135–41.
[22] Fan M, Bai J, Ding T. Adipose-derived stem cell transplantation inhibits vascular inflammatory responses and endothelial dysfunction in rats with atherosclerosis. Yonsei Med J 2019;60:1036–44.
[23] Rani S, Ryan AE, Griffin MD. Mesenchymal stem cell-derived extracellular vesicles: toward cell-free therapeutic applications. Mol Ther 2015;23:812–23.
[24] Shang D, Liu H, Tu Z. Pro-inflammatory cytokines mediating senescence of vascular endothelial cells in atherosclerosis. Fundam Clin Pharmacol 2023;37:928–36.
[25] Zheng Q, Yuan Y, Yi W. C1q/TNF-related proteins, a family of novel adipokines, induce vascular relaxation through the adiponectin receptor-1/AMPK/eNOS/nitric oxide signaling pathway. Arterioscler Thromb Vasc Biol 2011;31:2616–23.
[26] Wong GW, Krawczyk SA, Kitidis-Mitrokostas C. Identification and characterization of CTRP9, a novel secreted glycoprotein, from adipose tissue that reduces serum glucose in mice and forms heterotrimers with adiponectin. Faseb J 2009;23:241–58.
[27] Li J, Zhang P, Li T. CTRP9 enhances carotid plaque stability by reducing pro-inflammatory cytokines in macrophages. Biochem Biophys Res Commun 2015;458:890–5.
[28] Sun H, Zhu X, Zhou Y. C1q/TNF-Related protein-9 ameliorates ox-LDL-induced endothelial dysfunction via PGC-1alpha/AMPK-mediated antioxidant enzyme induction. Int J Mol Sci 2017;18.
[29] Yan Z, Cao X, Wang C. C1q/tumor necrosis factor-related protein-3 improves microvascular endothelial function in diabetes through the AMPK/eNOS/NO. signaling pathway. Biochem Pharmacol 2022;195:114745.
[30] Bartel DP. MicroRNAs: genomics, biogenesis, mechanism, and function. Cell 2004;116:281–97.
[31] Yu H, Cao H. MicroRNA-98 inhibition accelerates the development of atherosclerosis via regulation of dysfunction of endothelial cell. Clin Exp Hypertens 2023;45:2206068.
[32] Driscoll J, Patel T. The mesenchymal stem cell secretome as an acellular regenerative therapy for liver disease. J Gastroenterol 2019;54:763–73.
[33] Lou G, Chen Z, Zheng M. Mesenchymal stem cell-derived exosomes as a new therapeutic strategy for liver diseases. Exp Mol Med 2017;49:e346.
[34] Xiao X, Xu M, Yu H. Mesenchymal stem cell-derived small extracellular vesicles mitigate oxidative stress-induced senescence in endothelial cells via regulation of miR-146a/Src. Signal Transduct Targeted Ther 2021;6:354.
[35] Comarita IK, Vilcu A, Constantin A. Therapeutic potential of stem cell-derived extracellular vesicles on atherosclerosis-induced vascular dysfunction and its key molecular players. Front Cell Dev Biol 2022;10:817180.